Int. J. Heat Mass Transfer. Vol. 33, No. 4, pp. 673–681, 1990
Printed in Great Britain

0017–9310/90 $3.00 + 0.00

Two-phase flow and dryout in a screen wick saturated with a fluid mixture

D. A. PRUZAN, K. E. TORRANCE and C. T. AVEDISIAN
Sibley School of Mechanical and Aerospace Engineering, Cornell University, Ithaca, NY 14853, U.S.A.

(*Received* 28 *October* 1988 *and in final form* 6 *June* 1989)

Abstract—Experiments are performed to investigate the use of water–ethanol mixtures as a heat pipe coolant. An everted heat pipe structure consisting of a vertical tube, internally heated at the top, and around which is wrapped four layers of 325 mesh stainless steel screen, is used to measure the steady state and dryout heat fluxes as a function of mixture composition and capillary rise height. For small capillary rise heights it is observed that the maximum operating heat flux could be increased by 135% with water–ethanol mixtures as compared to pure water. As the capillary rise height is increased the performance of water–ethanol mixtures becomes comparable to that of pure water. The measured dryout heat fluxes for pure water and pure ethanol are in reasonable agreement with the predictions of an analytical model which allows for two-phase flow, boiling, and dryout in the heated section of the wick.

1. INTRODUCTION

ADVANCES in miniaturization of semiconductor chips have pushed to the limit the ability to dissipate by free/forced convection heat transfer the high operating heat fluxes that are encountered. Current chip heat fluxes of 20 W cm^{-2} are not uncommon coupled with chip temperatures of less than 373 K for reliable operation [1].

One device which has the potential for meeting the needs of the electronics industry for dissipating the high fluxes generated during operation of very high speed integrated circuit (VHSIC) chips is the heat pipe [2]. Its advantages in this regard are that (1) the coolant is self-contained in the heat pipe housing and therefore separated from the chip, thus mitigating problems of hermetic sealing, (2) there are no moving parts within the heat pipe, (3) heat pipes can be produced in a flat plate configuration [3–5] which is appropriate for attachment to multichip circuit board modules, and (4) the heat pipe is, theoretically at least [6], capable of meeting the projected cooling needs of future generations of chips. However, to dissipate the high fluxes characteristic of those generated in VHSIC chips, current heat pipes would require working fluids with unacceptably high operating temperatures. The problem is how to increase the heat flux without significantly increasing the operating temperature.

The present study explores the potential for using a mixture as the coolant within a heat pipe to extend its operating limits over that of a single component fluid. It is conjectured that the strong dependence of heat transfer rates on fluid composition characteristic of nucleate pool boiling (e.g. refs. [7, 8]) may extend to a liquid saturated wick in a heat pipe. While few studies have been carried out to explore the use of liquid/liquid mixtures in a heat pipe, Brommer [9] in particular has shown that mixtures can help the start-up behavior of heat pipes as well as create the potential for increased power levels. The interest in the present study was to examine the effect of fluid composition on the maximum or dryout heat flux (DHF). This heat flux is the highest steady state heat flux that a heat pipe can dissipate. At higher fluxes the mass evaporation rate exceeds the rate at which liquid can be resupplied by capillary action in the wick. The potential then exists for a severe degradation of performance of the device being cooled due to the subsequent wall temperature excursion above the DHF.

An everted heat pipe was used to examine the performance of fluid mixtures. This configuration was chosen for simplicity of design and because it allows direct visual access to the wick during operation [10–12]. The present design consisted of a wicking material wrapped around the outside of a vertical stainless steel tube which, in turn, was mounted within an outer glass shroud. The wick was composed of four layers of 325 mesh stainless steel screen tightly wrapped around the stainless steel tube. The fluid entered the wick from a pool surrounding the lower end of the tube, traveled up through an adiabatic length, and was vaporized by a heating element inside the top end of the wick/tube assembly. The fluids studied were water, ethanol, and water–ethanol mixtures. The pressure was 1 atm and the fluids were at their respective phase equilibrium temperatures corresponding to this pressure.

An analytical model is also presented which incorporates and extends previous single phase and boiling models for flow in a wicking structure [11, 13, 14]. The model provides further insight into the effect of wick properties on the boiling process of a single component fluid within the heated section of the wick.

NOMENCLATURE

D	inner diameter of annular wick
g	gravitational acceleration
h	heat transfer coefficient
h_{fg}	latent heat of vaporization
k	bulk permeability of the wick
k_l, k_v	relative permeabilities for liquid and vapor
L	distance from top of the heater to the liquid pool
L_h	heater length
P_l, P_v	local fluid pressures of liquid and vapor
P_c	capillary pressure
P_{sat}	saturation pressure of the fluid outside the wick
q''	heat flux
r_c	capillary radius of curvature
S	local liquid saturation
t	wick thickness
T	saturation temperature of the fluid
T_w	heater wall temperature
U	fluid superficial velocity in the x-direction within the wick
V	vapor superficial velocity in the y-direction within the wick
x, y	Cartesian coordinates (see Fig. 9)
X	ethanol concentration of the liquid phase
Y	ethanol concentration of the vapor phase.

Greek symbols

ε	porosity
μ_l, μ_v	dynamic viscosities of liquid and vapor, respectively
ρ_l, ρ_v	densities of liquid and vapor, respectively
σ	surface tension.

2. EXPERIMENT

A schematic of the experimental apparatus is shown in Fig. 1. It essentially consists of a wick wrapped around the outside of a vertically oriented stainless steel tube with the wick assembly in turn mounted within a glass chamber.

The chamber was made of a glass tube (10 cm i.d. by 46 cm tall) sealed at the top and bottom with stainless steel plates. A screen wick was wrapped around the outside of a 34 cm long, 1.28 cm o.d., thin-walled stainless steel tube. Physical parameters of the wick are listed in Table 1. Details of the heated section of the wick are shown in cross-section in Fig. 2. The heat source was a 0.64 cm diameter, 6.4 cm long electrical resistance heater which was press fit into an equal length, 1.23 cm o.d. copper sleeve. This arrangement approximated a spatially-uniform heat flux. The heater and copper sleeve were pressed into the top of the stainless steel tube, 1 cm from the top, as shown. The top of the tube was sealed with a Teflon O-ring and a stainless steel cap. The cap was held in position with a tension wire running from the chamber base plate, across the top of the cap, and back to the other side of the base plate. The applied heat flux was determined from simultaneous measurements of the voltage drop and current in the heater to an accuracy within about 5%. This uncertainty allows for heat conduction losses through the support tube and lead wires, and for the voltage drop in the lead wires. Further details are available in ref. [15]. Heater voltage was controlled with a variable autotransformer.

Heater wall temperatures were measured with nine chromel–alumel thermocouple probes (0.05 cm in diameter) inserted in lengthwise grooves on the outside of the copper sleeve (see Fig. 2). The nine probes were equally distributed around the circumference of

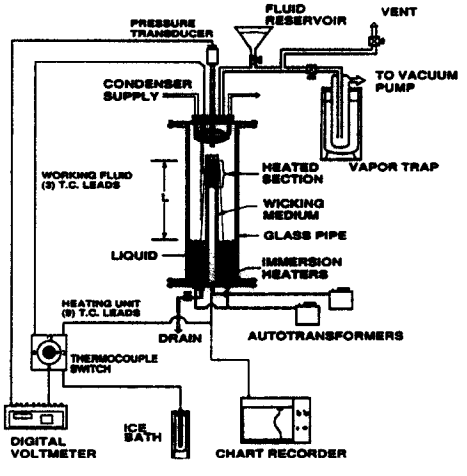

FIG. 1. Experimental apparatus for measuring wall superheat as a function of applied heat flux.

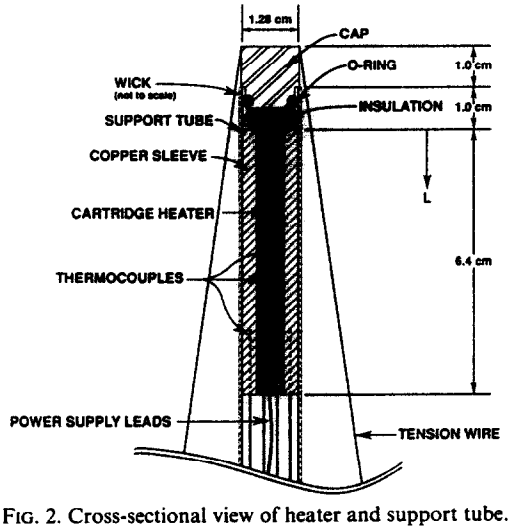

FIG. 2. Cross-sectional view of heater and support tube.

Table 1. Wick properties, four layer, 325 mesh stainless steel screen

Wick thickness, t (cm)	Permeability, k (cm^2)	Capillary radius, r_c (cm)	Porosity, ε (%)	Mounting tube diameter, D (cm)
0.0305	4.00×10^{-7}	2.77×10^{-3}	65	1.28

the sleeve with three each at the quarter, half, and three-quarter length positions of the sleeve. Working fluid temperatures in the test chamber were measured with three chromel–alumel thermocouple probes (0.10 cm in diameter) extending down from the upper plate. The three thermocouples were located at the top of the condenser coil (i.e. 2.5 cm down from the upper plate), at the midheight of the heated section (13.7 cm down from the upper plate), and at the midheight of the stainless steel tube (28.4 cm down from the upper plate). The uppermost thermocouple was on the centerline axis of the test chamber while the latter two thermocouples were approximately 1.0 cm radially away from the surface of the wick.

The superheat values reported are the difference between the average of the top three heating unit thermocouple readings and the average of the three working fluid thermocouple readings. The superheats reported are accurate to $\pm 2.5\%$ or better. To monitor temporal variations in heater wall temperature the output voltage of one of the three uppermost thermocouples in the heated section was recorded on a strip chart recorder.

The chamber was filled with the working fluid by first evacuating it with the aid of a vacuum pump and then drawing the test fluid into the chamber until the fluid reached the top of the heater. The fluid was boiled and periodically vented over a period of 2 h by using both the immersion and wick heaters, and was then allowed to cool overnight. This procedure minimized the trapping of non-condensible gases within the wick during the filling procedure. The fluid was alternately boiled and flashed momentarily to vacuum until the saturation temperature commensurate with the initially prepared fluid composition was reached. Fluid was then drained from the chamber until the desired L value (Fig. 1) was reached. Compositions of the fluid mixtures tested were inferred by comparing measured densities with tabulated handbook values [16] for water–ethanol mixtures. The fluids used (i.e. anhydrous ethanol (U.S.P.) and deionized and distilled water) were of liquid chromatography grade or better. Fluid densities were measured with a precision pipette and a digital laboratory scale to an uncertainty of $\pm 0.6\%$ mol % ethanol. The fluid compositions were measured during and after a run. Compositions were found to differ from the initially prepared mixture by less than 3%.

Vapor produced by the wick and immersion heaters (used to maintain the working fluid at saturation conditions) was condensed on the upper plate and the exposed region of the chamber wall. At high heat fluxes a condenser consisting of a coil of copper tubing supplied with coolant from a variable temperature circulating bath was activated. The condenser coil was designed so that no condensate could drip down onto the heated section of the wick. The pressure in the chamber was monitored with an electrical transducer connected to a digital voltmeter and was held constant at 1 atm to within $\pm 0.3\%$.

The dryout heat flux was measured by increasing the power to the heater in steps, insuring that steady state conditions had been reached between power increases, until either a wall temperature excursion of the uppermost thermocouples imbedded in the heater was noted, or the variation of applied heat flux with wall superheat revealed a noticeable change of slope. At low heat fluxes the heater wall temperature would eventually reach a steady value for the given heat flux as indicated by the one thermocouple output to the strip chart recorder. For higher heat fluxes near the dryout limit a steady output temperature was not achieved. Instead the recorded temperature rose slowly. This slow drift is attributed to a gradual increase with time of the size of the dryout zone in the wick. The rise in temperature of the one thermocouple charted was indicative of the overall rise in the average superheat with time. These rates were typically of the order of $2°C\ h^{-1}$ for both the pure fluids and the fluid mixtures.

3. EXPERIMENTAL RESULTS

Mixture compositions of 0, 2.3, 25, 50, and 100 mol % ethanol in water were tested. Capillary rise heights ranged from $L = 0$ (i.e. liquid to the top of the heater) to $L = 30$ cm. The range $0 < L < 6.4$ cm corresponds to partial immersion of the heater. A total of 24 combinations of composition and capillary rise height were studied. The 2.3% ethanol–water mixture was included because an earlier pool boiling model [17] and recent experiments on boiling from small-diameter wires [18] revealed a maximum in the critical heat flux near that composition.

The variation of measured wall superheats with applied heat flux is shown in Fig. 3 with L as the curve parameter. The data in Figs. 3(a)–(c) correspond to pure water, 2.3% ethanol–water, and 100% ethanol, respectively. Note that different scales are used for the three graphs. The superheat values reported are the difference between the average of the top three thermocouple readings within the heated section and the average of the three working fluid thermocouple readings.

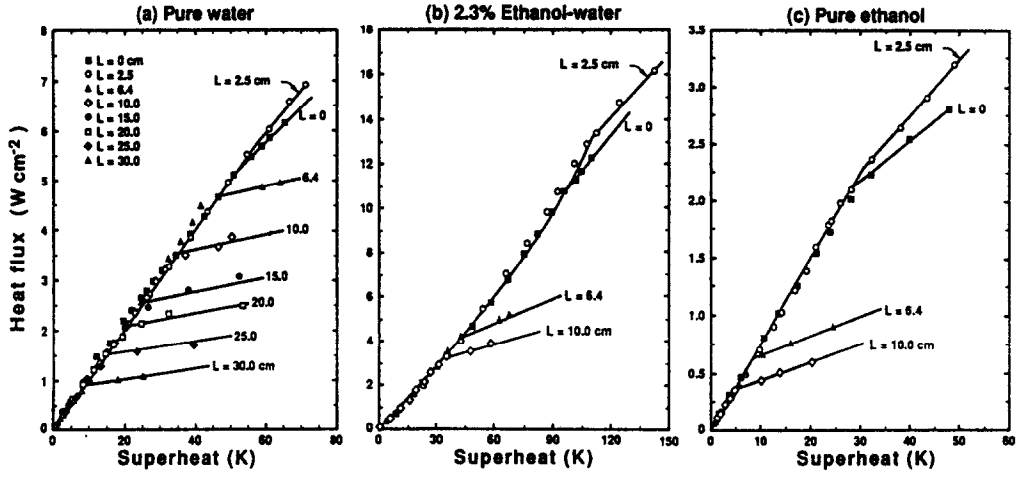

FIG. 3. Applied heat flux vs superheat for (a) pure water, (b) 2.3% ethanol–water, and (c) pure ethanol. The curve parameter is the capillary rise height, L.

In Fig. 3(a) each of the individual curves, corresponding to a specific value of L, displays a similar behavior. At low heat fluxes the measured superheats lie on a linear portion of the curve and at high heat fluxes the superheats again lie on a linear portion of the curve but with a lower slope. The change in slope of the curve is indicative of a change in the heat transfer mechanism within the wick and is taken to be the DHF. The change is less pronounced when the heater is fully submerged ($L = 0$) and partially submerged ($L = 2.5$ cm). The data for 2.3% ethanol–water and pure ethanol (Figs. 3(b) and (c), respectively) result in similarly shaped curves with the exception that the steady state portions of the curves in Fig. 3(b) (heat fluxes below DHF) are not linear.

The dryout heat fluxes for pure water, 2.3% ethanol–water, and 100% ethanol taken from Fig. 3 are cross-plotted as a function of capillary rise height in Fig. 4. Dryout heat fluxes for 10 cm $< L \leqslant$ 30 cm were measured for pure water only. The heater length of $L = 6.4$ cm is denoted by large ticks on the abscissae. For all mixtures studied the largest DHF occurred for a partially submerged heater ($L = 2.5$ cm). The dropoff in DHF for $L > 2.5$ cm is attributed to a lower capillary supply of fluid to the heated section. As L is increased, more of the capillary action is used to lift the fluid against gravity and less is available to sustain fluid flow through the wick. The reduction in DHF for $L < 2.5$ cm is attributed to the mutual interference of vapor and liquid flows in the liquid pool near the submerged heated section.

Dryout heat flux values for pure water (Fig. 4(a)) are considerably above those for pure ethanol (Fig. 4(c)) due in part to the lower latent heat of vaporization and surface tension of the latter. The binary boiling process appears to overcome the lower latent heat of vaporization and surface tension for the 2.3% ethanol–water mixture resulting in a peak DHF value that is 2.35 times larger than the peak value for pure water at $L = 2.5$ cm.

In the region below the DHF points in Fig. 3, a single curve for each composition adequately describes the behavior for all L values. This suggests that the steady state heat transfer coefficient h, defined by the ratio $q''/\Delta T$, is independent of L, a trend also observed by Abhat and Seban [10]. Further, for pure

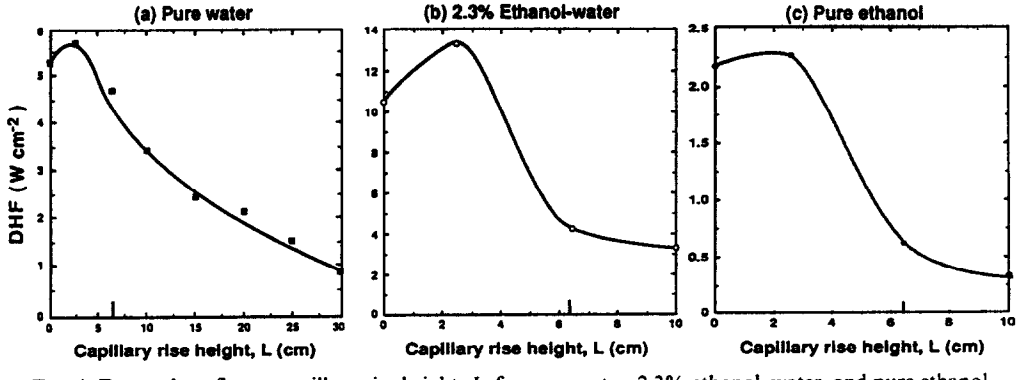

FIG. 4. Dryout heat flux vs capillary rise height, L, for pure water, 2.3% ethanol–water, and pure ethanol. Dryout heat flux data are taken from Fig. 3.

water (Fig. 3(a)) and pure ethanol (Fig. 3(c)), a linear behavior of q'' vs ΔT is observed. The respective h values of 0.11 and 0.074 W cm^{-2} K^{-1} are thus independent of superheat temperature. For the 2.3% ethanol–water mixture the heat transfer coefficient increases with increasing heat flux; the corresponding h values range from 0.080 to about 0.10 W cm^{-2} K^{-1} as q'' varies from 0 to 10 W cm^{-2}.

The lower heat transfer coefficients for ethanol and ethanol–water mixtures as compared to pure water lead to higher superheats for a given heat flux, but not necessarily to higher heater wall temperatures. The heater wall temperature is the sum of the superheat and the saturation temperature, and for water–ethanol mixtures the saturation temperature drops rapidly as small concentrations of ethanol are added to water [18]. To illustrate these effects, the variations in heat transfer coefficient and heater wall temperature with percent ethanol are shown in Fig. 5. Results are shown for $q'' = 2.00$ W cm^{-2} and are normalized by the corresponding values for pure water. Data were taken from Fig. 3, and from similar graphs for the other mixture compositions studied. While a minimum in the heat transfer coefficient occurs at approximately 25% ethanol, which agrees with results obtained by Tolubinskiy and Ostrovskiy [19] for pool boiling on a 0.45 cm diameter vertical tube, the heater wall temperature monotonically decreases with increasing ethanol concentration.

Cross plots of DHF vs capillary rise height, L, and mixture composition are shown in Figs. 6 and 7, respectively. For L between 0 (corresponding to pool boiling on a vertical cylinder covered with four layers of a 325 screen mesh) and about 5.9 cm (partially submerged heater) the 2.3% ethanol–water mixture DHF values are greater than those for pure water.

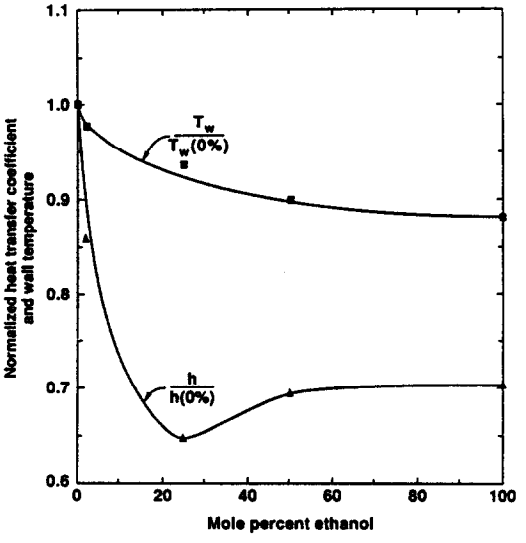

FIG. 5. Heat transfer coefficient and wall temperature both normalized with corresponding values for pure water, plotted against mol % ethanol.

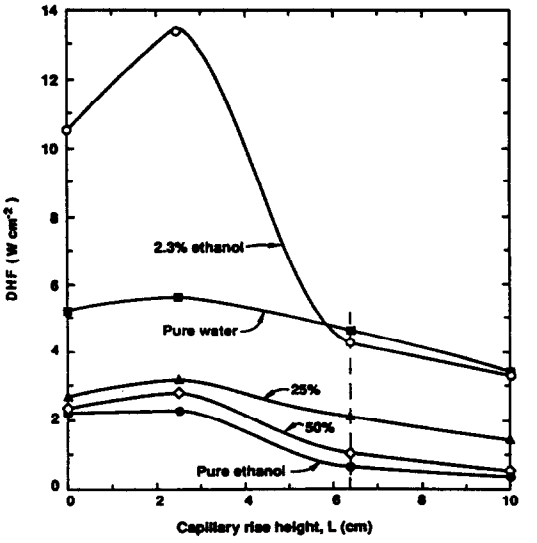

FIG. 6. Dryout heat flux vs capillary rise height, L, for all ethanol–water compositions tested. Dashed line denotes heater length, $L = 6.4$ cm.

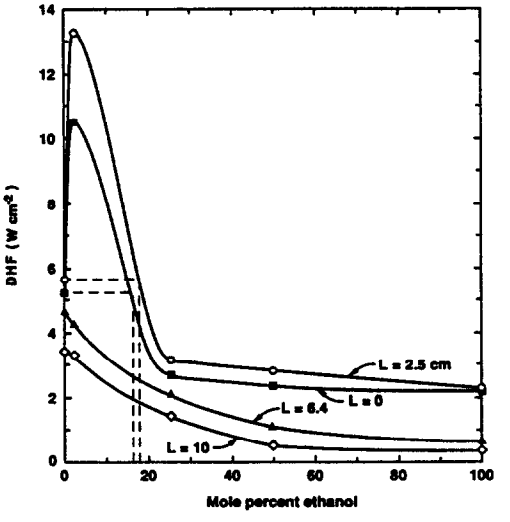

FIG. 7. Dryout heat flux as a function of mol % ethanol. Horizontal dashed lines for $L = 0$ and 2.5 cm suggest a range of ethanol–water concentrations for which DHF is above that for pure water.

At larger rise heights the significantly lower surface tension of the 2.3% mixture as compared to pure water results in a lower capillary supply of fluid to the heater and thus a lower DHF. In Fig. 7, the ranges of concentrations of ethanol that lead to DHF values greater than those for pure water are shown by dashed lines. For $L = 0$ the range of concentrations extends from 0% ethanol to about 16.7% ethanol; for $L = 2.5$ cm the range extends to 18.0% ethanol. The 2.3% ethanol–water mixture proved to be the best of the limited set of mixtures tested.

As previously noted, the 2.3% ethanol–water mixture was chosen based on prior analytical and exper-

imental studies of binary pool boiling [17, 18]. A pool boiling model estimated the peak critical heat flux to occur for a liquid phase concentration, X, where the associated value of $(dT/dX)(Y-X)$ is a maximum [17]. On a graph of saturation temperature vs percent ethanol, as shown in Fig. 8 from ref. [18], dT/dX is the slope of the liquid phase curve at a concentration X, and $(Y-X)$ is the difference in vapor and liquid phase concentrations at the saturation temperature corresponding to the liquid phase concentration X. For ethanol–water at 1 atm, $(dT/dX)(Y-X)$ reaches a maximum at roughly $X = 3.1\%$. An experimental study of binary pool boiling on small diameter horizontal wires with ethanol–water mixtures revealed that the critical heat flux was a maximum near this value of X [18]. For the three smallest diameter wires tested, 0.0510, 0.0767 and 0.1016 cm, the respective peak critical heat fluxes occurred at an average concentration of 2.3% ethanol–water. Therefore, this mixture concentration was selected for inclusion in the present study.

It is noted that of the 24 combinations of composition and capillary rise height tested, 9 were duplicated more than once with an average deviation in DHF of less than 4%.

4. ANALYSIS

Several analytical models have been proposed to predict the dryout heat flux for single component fluids in a heat pipe [10, 11, 13, 14]. We use the most recent of these models [14] and extend it to include features not previously used in heat pipe models. The discussion is restricted to single-component fluids.

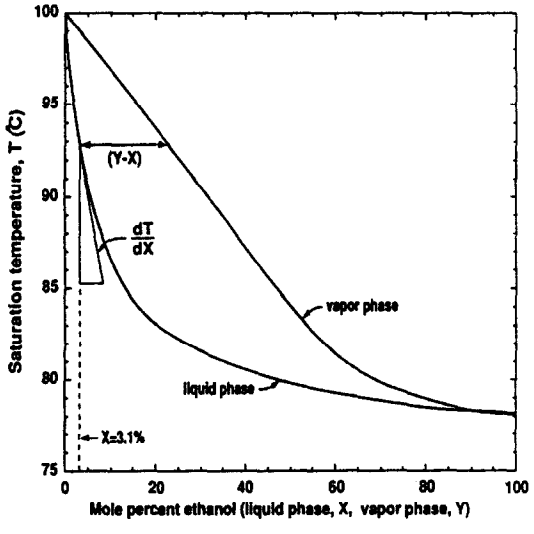

FIG. 8. Saturation temperature (T) vs mol % ethanol for ethanol–water mixtures at 1 atm. X and Y denote the mol % ethanol in the liquid and vapor phases, respectively. The quantity $(dT/dX)(Y-X)$ reaches a maximum value at $X = 3.1\%$.

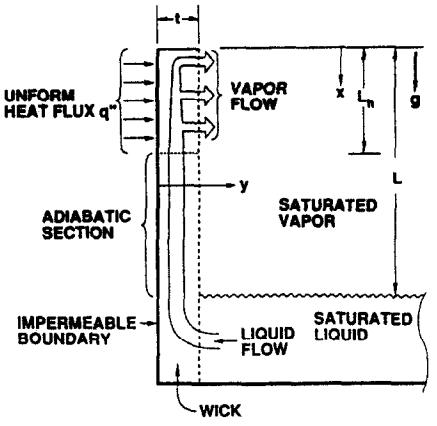

FIG. 9. Geometry of heat pipe considered in the analytical model.

A Cartesian, two-dimensional geometry as sketched in Fig. 9 is used as a basis for the present model. Such a model is a satisfactory approximation of a cylindrical wick when the wick thickness/diameter ratio, t/D, is small [15] (which corresponds to the present experimental condition as shown in Table 1). The wick is shown in cross-section and is of wick thickness t, with an impermeable boundary at $y = 0$ and a permeable boundary at $y = t$. Fluid from the liquid pool enters through the permeable face and is drawn vertically upward against gravity to the heated section by the capillary action of the wick. A uniform heat flux applied over the heater length, L_h, boils the liquid. The ensuing vapor flows horizontally out of the wick.

The model assumes that all system variables are functions of the x coordinate only and that all fluid properties are constant. The one-dimensional flow of liquid in the adiabatic section is of constant velocity throughout the adiabatic length and is governed by the Darcy momentum equation

$$U = -(k/\mu_l)[dP_l/dx - \rho_l g] \tag{1}$$

where U is the Darcy or superficial fluid velocity.

Two-phase flow occurs in the heated section. Following Singh and Shaubach [14], liquid flow is assumed to be one-dimensional in the vertical direction, with a one-dimensional crossflow of vapor in the y-direction. The governing equations are the continuity, energy, and Darcy momentum equations for two-phase flow in a porous structure, equations (2), (3) and (4), respectively

$$\rho_v V = \rho_l t\, dU/dx \tag{2}$$

$$q'' = \rho_v V h_{fg} \tag{3}$$

$$U = -(kk_l/\mu_l)[dP_l/dx - \rho_l g] \tag{4a}$$

$$V = (kk_v/\mu_v)[(P_v - P_{sat})/t]. \tag{4b}$$

The heating rate q'' is assumed to give rise to a vapor velocity V through equation (3). With q'' constant, V is constant over the vertical height of the heated

section. The velocity U and the pressures P_l and P_v must satisfy equations (2) and (4) locally. Of course, overall continuity requires that the vertical flow rate of liquid in the adiabatic section must balance the production of vapor in the heated section.

Additional information is needed to prescribe k_l, k_v, P_l and P_v. Frequently used functional forms are [20]

$$k_l = S^3 \tag{5a}$$

$$k_v = (1-S)^3 \tag{5b}$$

$$P_v - P_l = P_c = 2\sigma/r_c. \tag{6}$$

Several fluid and wick parameters must be specified in equations (1)–(6). Physical properties for water and ethanol were taken from ref. [16]. The capillary radius of curvature r_c was determined from independent static 'hold up' height experiments, and the bulk permeability k was inferred from measured dryout data at large values of the capillary rise height. Under conditions of large capillary head, the pressure drop due to two-phase effects (i.e. mutual interference of liquid and vapor flows in the heated section of the wick) can be neglected in comparison with the pressure drop due to pure liquid flow in the adiabatic section. This assumption results in a single phase model relating DHF to the quantity $1/(L-L_h/2)$ plus fluid and wick properties. With the other wick properties known this single phase model can be fit to the experimental data to determine the bulk permeability, k. Also, a porosity ε can be inferred from k and r_c with the Kozeny–Carman formula [21]. The measured and inferred physical parameters for the four layer screen wick used in the experiments are listed in Table 1. Further details are given in ref. [15].

Equation (1) was solved analytically in the adiabatic section, and equations (2)–(6) were solved numerically in the heated section. Finite difference methods were used with an adjustable step size to help ensure uniform spatial accuracy. The solution was marched from the base of the heated section (where the saturation was 100% and liquid velocity and pressure were known from the solution of equation (1)) to the top of the heated section. Dryout heat flux conditions were assumed to exist when the liquid saturation was 1% or less at the top of the heated section.

Using the analytical–numerical model described in the previous section, DHF values for single component fluids were determined as a function of the capillary rise height, L. The results are shown by dashed lines in Fig. 10. Also shown are experimentally measured DHF values for pure water and pure ethanol from Fig. 4. The solid lines are best fit curves through the experimental data. The experimental and theoretical results are in reasonable agreement. The analysis overpredicts the DHF for water when $L < 18$ cm and slightly underpredicts in the range 18 cm $< L < 30$ cm. The theoretical DHF values for pure ethanol slightly underpredict the experimental results, but the trends are otherwise similar. Previous single

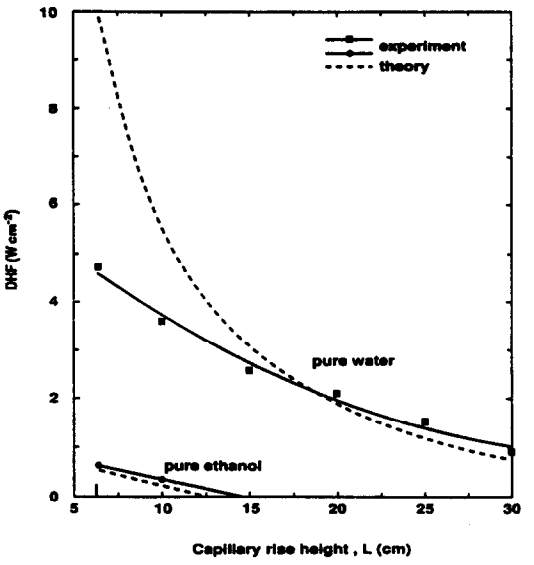

FIG. 10. Theoretical and experimental DHF values as a function of capillary rise height, L, for pure water and pure ethanol. Experimental data are taken from Fig. 4.

phase analytical models [11, 13] which assumed a fully saturated wick were found to substantially overpredict the DHF values for water and for ethanol for small L's as compared to the present model.

Dryout heat flux predictions from the analytical model depend on three geometric parameters of the wick; namely, the wick thickness, t, permeability, k, and capillary radius of curvature, r_c. For a wrapped screen wick there is uncertainty in all three parameters. Accordingly, a sensitivity study was carried out. A change of 10% in any one of these parameters was found to influence the analytical curves in Fig. 10 by 10% or less.

The analytical results are also sensitive to the form of the relative permeability and capillary pressure equations used. For the wick tested, equations (5) and (6) appear to be the most appropriate formulations. The differences between the analytical and experimental results shown in Fig. 10 are likely due to dissimilarities in the internal geometry of the screen wick and a truly uniform porous structure (on which the analysis was based). Additional work with sintered copper wicks shows better agreement between analysis and experiment and will be presented in a future paper. No attempt was made to extend the current analysis to ethanol–water mixtures due to a lack of theoretical models for the binary boiling process compatible with the one-dimensional boiling-flow model used here.

5. CONCLUSIONS

The present experiments provide information on the effect of ethanol–water mixtures on heat pipe performance. Under certain conditions a significant increase in the maximum heat transfer rate can be

achieved by adding a small amount of ethanol to water. Although the binary boiling process may lead to an improvement in the heat transfer mechanism, any reductions in surface tension for the mixture should be avoided as this reduces the capillary pumping capability of the wick and limits heat pipe performance at large capillary rise heights.

The present analytical model allows a prediction of the maximum heat transfer rate for heat pipes filled with a single component fluid. Predictions from the model are in reasonable agreement with experimental results. Future work should include an extension of the model to binary boiling systems.

Acknowledgements—The authors thank Mr Algerd Basiulis of Hughes Aircraft and Dr Roop Mahajan of AT&T for helpful discussions during the course of this work. The contributions of P. Vallone, M. North and C. Riley during the design and operation of the experiment are also acknowledged. This work formed part of a project supported by the Semiconductor Research Corporation under Project Nos. 86-01-070-02 and 87-MP-070-02. Additional support under NSF grant No. CBT-8451075 was also appreciated.

REFERENCES

1. R. Hannemann, F. P. Incropera and R. Simons, *Research Needs in Electronic Cooling* (Edited by F. P. Incropera). National Science Foundation, Washington, DC (1986).
2. L. Waller, An old idea may solve VHSIC cooling problem, *Electronics* 19–20 (5 August 1985).
3. G. W. Scott and H. J. Tanzer, Evaluation of heat pipes for conduction-cooled level II avionic packages, *Heat Transfer Engng* **9**, 32–43 (1988).
4. A. Basiulis, H. Tanzer and S. McCabe, Thermal management of high power PWBs through the use of heat pipe substrates, *Proc. Sixth Annual Int. Electronics Packaging Conf.*, San Diego, California (1986).
5. P. V. Ciekurs, An approach to solving the hot spot cooling problem in electronic packaging, ASME Paper No. 86-WA/EEP-1 (1986).
6. C. L. Tien, Fluid mechanics of heat pipes, *Ann. Rev. Fluid Mech.* **7**, 167–185 (1975).
7. S. J. D. Van Stralen, The mechanism of nucleate boiling in pure liquids and in binary fluids, *Int. J. Heat Mass Transfer* **9**, 995–1046 (1966).
8. D. J. Purdy and C. T. Avedisian, Critical heat flux in fluid mixtures, Energy Report No. E-87-02, Cornell University, Sibley School of Mechanical and Aerospace Engineering, Ithaca, New York (1987).
9. H. J. Brommer, Theoretical and experimental investigation of two-component heat pipes, AIAA Paper No. 74-720 (1974).
10. A. Abhat and R. A. Seban, Boiling and evaporation from heat pipe wicks with water and acetone, *J. Heat Transfer* **96**, 331–337 (1974).
11. K. R. Chun, Some experiments on screen wick dry-out limits, *J. Heat Transfer* **94**, 46–51 (1972).
12. P. J. Marto and W. L. Mosteller, Effect of nucleate boiling on the operation of low temperature heat pipes, ASME Paper No. 69-HT-24 (1969).
13. C. Roberts and K. Feldman, Predicting performance of heat pipes with partially saturated wicks, ASME Paper No. 72-WA/HT-38 (1972).
14. B. S. Singh and R. M. Shaubach, Boiling and two-phase flow in the capillary porous structure of a heat pipe. In *Multiphase Transport in Porous Media*, HTD-Vol. 91, pp. 61–68. ASME, New York (1987).
15. D. A. Pruzan, Experimental and analytical investigations into enhanced peak boiling heat transfer from capillary fed porous media, Ph.D. Thesis, Cornell University, Sibley School of Mechanical and Aerospace Engineering, Ithaca, New York (1989).
16. *CRC Handbook of Chemistry and Physics* (Edited by R. C. Weast) (67th Edn), p. D-228. CRC Press, Boca Raton, Florida (1986–1987).
17. S. J. D. Van Stralen, The boiling paradox in binary liquid mixtures, *Chem. Engng Sci.* **25**, 149–171 (1970).
18. R. P. Reddy, The critical heat flux in binary mixtures of water and ethanol, M.S. Thesis, University of Houston, Department of Mechanical Engineering, Houston, Texas (1987).
19. V. I. Tolubinskiy and Yu. N. Ostrovskiy, Mechanism of heat transfer in boiling of binary mixtures, *Heat Transfer—Sov. Res.* **1**, 6–11 (1969).
20. M. R. J. Wyllie, Relative permeability. In *Petroleum Production Handbook* (Edited by T. C. Frick), Vol. 2, Chap. 25. McGraw-Hill, New York (1962).
21. J. Bear, *Dynamics of Fluids in Porous Media*, p. 166. American Elsevier, New York (1972).

ECOULEMENT DIPHASIQUE ET ASSECHEMENT DANS UNE MECHE EN GRILLAGE SATUREE PAR UN MELANGE DE FLUIDES

Résumé—Des expériences sont conduites pour étudier l'utilisation des mélanges eau–éthanol comme liquide de caloduc. Une structure de caloduc consiste en un tube vertical chauffé en bout de façon interne et entouré de quatre couches de grillages en acier inox est utiilisé pour mesurer des flux thermiques d'état stationnaire et d'assèchement en fonction de la composition du mélange et de la hauteur de la montée capillaire. Pour les faibles ascensions capillaires, on observe que le flux thermique maximal opératoire peut être augmenté de 135% avec des mélanges eau–éthanol par rapport à l'eau pure. Lorsque la hauteur augmente, la performance des mélanges eau–éthanol devient comparable à celle de l'eau pure. Les flux thermiques d'assèchement mesurés pour l'eau pure et pour l'éthanol pur sont en accord raisonnable avec les prédictions d'un modèle analytique qui, pour l'écoulement diphasique, concerne l'ébullition et l'assèchement dans la section chaude de la mèche.

ZWEIPHASENSTRÖMUNG UND DRYOUT IN EINEM MIT EINEM FLÜSSIGKEITSGEMISCH GESÄTTIGTEN DRAHTDOCHT

Zusammenfassung—Es werden Experimente durchgeführt, um die Verwendung von Gemischen aus Wasser und Ethanol als Arbeitsmittel für Wärmerohre zu untersuchen. Es wird eine nach außen gewendete Wärmerohrstruktur verwendet. Die Anordnung besteht aus einem senkrechten Rohr, welches am oberen Ende innen beheizt wird und um welches vier Lagen eines Edelstahlgewebes mit 325 Maschen je Zoll gewickelt ist. Es wird die Wärmestromdichte im stationären Zustand und beim Dryout in Abhängigkeit von der Zusammensetzung des Gemisches und der kapillaren Steighöhe gemessen. Es wird festgestellt, daß bei kleinen kapillaren Steighöhen die maximale Betriebswärmestromdichte mit Wasser–Ethanol-Gemischen um 135% gegenüber reinem Wasser gesteigert werden kann. Mit zunehmenden kapillaren Steighöhen wird der Wirkungsgrad bei Wasser–Ethanol-Gemischen ähnlich dem bei reinem Wasser. Die gemessenen Wärmestromdichten bei Dryout stimmen für reines Wasser und reines Ethanol gut mit den Berechnungen nach einem analytischen Modell überein, welches die Zweiphasenströmung, das Sieden und den Dryout im beheizten Bereich des Dochtes berücksichtigt.

ДВУХФАЗНОЕ ТЕЧЕНИЕ И КРИЗИС КИПЕНИЯ В ФИТИЛЕ, НАСЫЩЕННОМ СМЕСЬЮ ЖИДКОСТЕЙ

Аннотация—Проведено экспериментальное исследование возможности использования водо-этаноловых смесей в качестве теплоносителей для тепловой трубы. "Перевернутая" капиллярная структура тепловой трубы состоит из вертикальной трубки, нагреваемой внутренним источником тепла у верхнего торца и обернутой 4 слоями сетки с 325 ячейками на один линейный дюйм, изготовленной из нержавеющей стали. Измерялись величины тепловых потоков в стационарном режиме и при кризисе кипения в зависимости от состава смеси и высоты капиллярного подъема жидкости. Найдено, что при малых значениях последней максимальную величину теплового потока можно увеличить на 135%, если вместо чистой воды использовать водо-этаноловую смесь. С ростом высоты капиллярного подъема эта разница нивелируется. Измеренные значения тепловых потоков при кризисе кипения чистой воды и чистого этанола хорошо согласуются со значениями, рассчитываемыми по аналитической модели с учетом двухфазного характера потока, кипения и кризиса кипения в нагреваемой части фитиля.